Scientific Research Publishing

Journal of Applied Mathematics and Physics, 2018, 6, 667-676
http://www.scirp.org/journal/jamp
ISSN Online: 2327-4379
ISSN Print: 2327-4352

Numeric and Analytic Investigation on Phase Diagrams and Phasetransitions of the $\nu = 2/3$ Bilayer Fractional Quantum Hall Systems

Y. D. Zheng, T. Sorita

Research and Development Department, Mitsubishi Electric (China) Company Limited, Shanghai, China
Email: zhengyd09@163.com

How to cite this paper: Zheng, Y.D. and Sorita, T. (2018) Numeric and Analytic Investigation on Phase Diagrams and Phasetransitions of the $\nu = 2/3$ Bilayer Fractional Quantum Hall Systems. *Journal of Applied Mathematics and Physics*, **6**, 667-676.
https://doi.org/10.4236/jamp.2018.64060

Received: March 19, 2018
Accepted: April 9, 2018
Published: April 12, 2018

Abstract

The phase diagrams and phase transitions of a typical bilayer fractional quantum Hall (QH) system with filling factor $\nu = 2/3$ at the layer balanced point are investigated theoretically by finite size exact-diagonalization calculations and an exactly solvable model. We find some basic features essentially different from the bilayer integer QH systems at $\nu = 2$, reflecting the special characteristics of the fractional QH systems. The degeneracy of the ground states occurs depending on the difference between intralayer and interlayer Coulomb energies, when interlayer tunneling energy (Δ_{SAS}) gets close to zero. The continuous transitions of the finite size systems between the spin-polarized and spin-unpolarized phases are determined by the competition between the Zeeman energy (Δ_Z) and the electron Coulomb energy, and are almost not affected by Δ_{SAS}.

Keywords

Bilayer Fractional Quantum Hall Systems, Phase Diagrams, Phase Transition, Exactdiagonalization, Exactly Solvable Model

1. Introduction

Quantum Hall (QH) effect [1] [2] [3] [4] [5], which rivals superconductivity in its fundamental significance, has attracted a great deal of experimental and theoretical interest since its discovering. Especially, fractional QH (FQH) systems exhibit a variety of many body quantum phenomena, due to the complete domination of the electron Coulomb interactions. In a more complicated case, the bilayer QH systems with both spin and layer (pseudospin) degrees of freedom, four sub energy levels are formed in the lowest Landau level (LLL), and the

ground states are to be determined by various factors such as interlayer/intralayer Coulomb energies (Δ_C), Zeeman energy (Δ_Z), interlayer tunneling energy (Δ_{SAS}) and bias energy (Δ_{bias}), etc. One expects reasonably that there exist rich quantum phases and many novel properties in the systems [6] [7].

The bilayer QH systems with filling factor $\nu = 2/m$ should be of the same type for any odd integer m. In this type of systems, the spin and pseudospin indices compete with each other, and the ground states are quite nontrivial because there are several ways to fill electrons into two sub energy levels in the LLL. Up to now, most of theoretical studies have focused on the $\nu = 2$ bilayer integer QH (IQH) systems based on Hartree-Fock analysis [8] [9] [10] [11] [12] [13], effective bosonic spin theory [14] [15], exact-diagonalization calculations [16] as well as effective quantum field theory, and have identified three phases, the ferromagnetic (FM), the symmetric (SYM) and the canted antiferromagnetic (CAF) phases in the ground states. On the other hand, the $\nu = 2/3$ bilayer QH system is a typical bilayer FQH system of this type, and can be regard as a best example of strongly correlated two-dimensional electron system for investigating the interplay of those entangled energy factors indicated above. However, even the basic problems, the ground states and the basic phase diagram of the $\nu = 2/3$ system are still leaved uninvestigated from the theoretical viewpoint. Because of the existence of the degeneracy in the ground state as indicated below, in many cases, the $\nu = 2/3$ bilayer QH system cannot simply be mapped to the $\nu = 2$ bilayer QH system based on the composite-fermion picture, and must be investigated directly by the microscopic theories and the numerical calculations.

Motivated by the present situation mentioned above, as the first step, in this paper, we employ the numerical and traditional analytic methods to investigate the finite size bilayer FQH systems. We report on some basic features of the ground states in the $\nu = 2/3$ bilayer QH systems at the layer balanced point ($\Delta_{bias} = 0$) and provide evidential quantitative results from exact-diagonalization (ED) [16] [17] [18] [19] [20] numerical calculations and analytic approaches carried out at $\nu = 2/3$. These features are essentially different from those in the $\nu = 2$ systems, and reflect the special characteristics of the bilayer FQH systems. 1) At $\nu = 2/3$, because the number of electrons is less than that of Landau sites in one sub energy level, in the small Δ_{SAS} limit, the degeneracy of the ground states occurs depending on the relative strength of the intralayer and interlayer Coulomb energies. Contrarily, at $\nu = 2$, because two sub energy levels in the LLL are filled by electrons, the ground states are non-degenerate even if Δ_{SAS} vanishes. 2) At least, the spin-polarize (SP) and spin-unpolarized (SU) phases exist in the $\nu = 2/3$ bilayer QH systems. The phase transitions between them are continuous in the finite size systems, and are determined by the competition between Δ_Z and Coulomb energy Δ_C, not that between Δ_Z and Δ_{SAS}, as in the $\nu = 2$ systems. The experimental results so far seem to support the conclusions above.

2. Exact-Diagonalization Method

We choose a finite size system with rectangular geometry for ED calculations.

Periodic boundary conditions are imposed on the rectangular cell of area $a \times b$ along the x and y axes, with the periodicities a and b, respectively. For simplicity, Landau level mixing and finite thickness of the system are not considered. Within the LLL, the Hamiltonian at the layer balanced point is described by Equations (1) and (2) as follows:

$$\hat{H} = \hat{H}_{\mathrm{t}} + \hat{H}_{\mathrm{z}} + \hat{H}_{\mathrm{int}},$$

$$\hat{H}_{\mathrm{t}} = -\frac{\Delta_{\mathrm{SAS}}}{2}\sum_{j\sigma}\left(\hat{c}^{+}_{jf\sigma}\hat{c}_{jb\sigma} + \hat{c}^{+}_{jb\sigma}\hat{c}_{jf\sigma}\right),$$

$$\hat{H}_{\mathrm{Z}} = -\frac{\Delta_{\mathrm{Z}}}{2}\sum_{j\mu}\left(\hat{c}^{+}_{j\mu\uparrow}\hat{c}_{j\mu\uparrow} - \hat{c}^{+}_{j\mu\downarrow}\hat{c}_{j\mu\downarrow}\right),$$

$$\hat{H}_{\mathrm{int}} = \frac{1}{2}\sum_{j_1-j_4}\sum_{\mu_1-\mu_4}\sum_{\sigma_1\sigma_2} V_{j_1j_2j_3j_4}\left(F_{\mu_1\mu_2\mu_3\mu_4}\right)\times \hat{c}^{+}_{j_1\mu_1\sigma_1}\hat{c}^{+}_{j_2\mu_2\sigma_2}\hat{c}_{j_3\mu_3\sigma_2}\hat{c}_{j_4\mu_4\sigma_1}, \quad (1)$$

$$V_{j_1j_2j_3j_4}\left(F_{\mu_1\mu_2\mu_3\mu_4}\right) = \frac{e^2}{4\pi\varepsilon}\frac{1}{2ab}\delta'\left(j_1+j_2, j_3+j_4\right)\sum_{s(q\neq 0)} e^{-i2\pi\frac{s(j_1-j_3)}{M}}\left[\frac{2\pi}{q}e^{-q^2l_{\mathrm{B}}^2/2}F_{\mu_1\mu_2\mu_3\mu_4}\right]_{q_x=\frac{2\pi}{a}s, q_y=\frac{2\pi}{b}(j_4-j_1)},$$

$$F_{ffff} = F_{bbbb} = 1, \quad F_{fbbf} = F_{bffb} = e^{-qd}, \text{ otherwise } \quad F_{\mu_1\mu_2\mu_3\mu_4} = 0, \quad (2)$$

where $\hat{H}_{\mathrm{t}}$, $\hat{H}_{\mathrm{z}}$ and $\hat{H}_{\mathrm{int}}$ represent the interlayer tunneling energy, Zeeman energy and two-body Coulomb interaction energy terms, respectively. $\hat{c}^{+}_{j\mu\sigma}$ ($\hat{c}_{j\mu\sigma}$) denotes electron creation (annihilation) operator. $j > 0$ is the y-direction momentum (Landau site) index (y-direction momentum $j_y = j - 1$), μ = f, b is the layer index that labels the front and back layers, and the spin denotation σ = ↑, ↓ represents the up and down spins. The coefficients in the $\hat{H}_{\mathrm{int}}$ term are given by Equation (2) [17] [18], where l_{B} means the magnetic length, d is the layer separation, q_{x} (q_{y}) indicates the single-electron wave numbers in x(y) direction. We define M as the degeneracy of the single Landau level. Only when $j_1 = j_2$ (mod M), $\delta'(j1, j_2) = 1$, otherwise, $\delta'(j_1, j_2) = 0$.

The total number of electrons in the system is defined by N_{e}. The N_{e}-electron basis vector is expressed by $\varphi_r = \hat{c}^{+}_{j_1\mu_1\sigma_1}\hat{c}^{+}_{j_2\mu_2\sigma_2}\ldots\hat{c}^{+}_{j_{Ne}\mu_{Ne}\sigma_{Ne}}|0\rangle$ (e.g., {2f ↑, 3b ↑, 5f ↓, 6b ↓} = $\hat{\mathbf{c}}^{+}_{2f\uparrow}\hat{\mathbf{c}}^{+}_{3b\uparrow}\hat{\mathbf{c}}^{+}_{5f\downarrow}\hat{\mathbf{c}}^{+}_{6b\downarrow}|0\rangle$ in the four-electron system). The number of the basis vectors is calculated to be $C_{4M}^{N_{\mathrm{e}}}$, which gives the dimension of the Hamiltonian matrix (H matrix). Diagonalization process of the H matrix can be simplified by reducing its dimension with the help of several symmetries in the system. Owing to the translational symmetry along the x (y) axis, the Hamiltonian conserves the total momentum J_{x} (J_{y}) in the x (y) direction [17] [18] [19] [20]. Along the y axis, for instance, $J_{\mathrm{y}} = \sum_{n=1}^{N_{\mathrm{e}}} j_{\mathrm{n}} \left(\mathrm{mod}\, M\right)$ is conservative, hence the H matrix as well as the basis vectors can be divided into M independent blocks corresponding to M different values of J_{y}, the dimension of the blocks are merely $1/M$ of that of the original H matrix [17] [18]. Let the common factor of N_{e} and M be C. Then, the H matrix can be divided into independent $M \times C$ blocks with different combination of (J_{x}, J_{y}), $J_x, J_y \in [0, C-1]$, correspondingly, and its di-

mension is reduced to about 1/MC. The wave vector in the system is defined by $\mathbf{k}=\left(k_x,k_y\right)=\left(J_x 2\pi/a, J_y 2\pi/b\right)$ [17] [18] [19]. Since the z-component of the total spin (S_z) is conserved in the system, each block above can be divided further into $N_e + 1$ independent blocks keeping S_z from $-N_e/2$ to $N_e/2$, respectively. In the ED calculations, we compute the matrix elements of these blocks and diagonalize them numerically. The aspect ratio a/b is fixed at 1.0.

In this study, a finite size $\nu = 2/3$ bilayer QH systems containing four electrons is chosen to execute the ED calculations. Henceforth, in the numerical results, the length and energy units are selected by l_B and Coulomb energy scale $E_C = e^2/4\pi\varepsilon l_B$, respectively.

3. Numerical Results and Discussion

The low-lying energy spectra of the $\nu = 2/3$ bilayer QH system with the fixed $d = 1.0$ for several values of Δ_{SAS} and Δ_Z are presented in **Figure 1**. The energies are plotted by different marks indicating different total spins S_z, and are measured from the ground-state energies indicated by arrows. Wave vectors k are normalized as kl_B, and (J_x, J_y) combinations contained in k are also represented. It

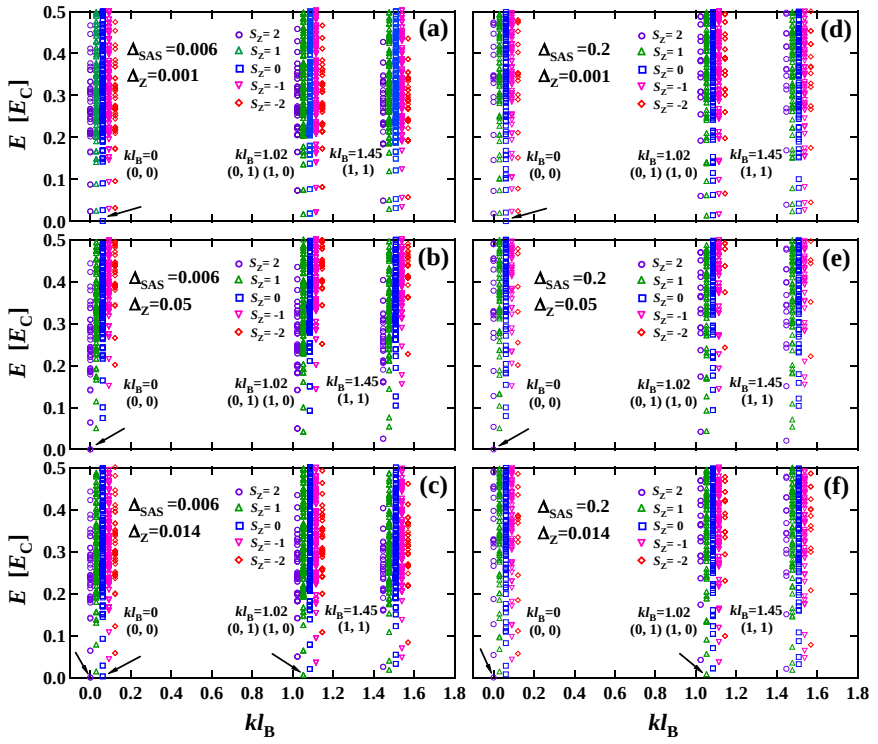

Figure 1. Energy spectrum of finite size ν = 2/3 bilayer QH systems (four electrons) for several values of Δ_{SAS} and Δ_Z at fixed $d = l_B$. Eigenenergies are in unit of (l_B is the magnetic length), and are plotted by different marks indicating different total spins S_z (leaving space between the neighboring S_z in the same k for clarity). The wave number k, normalized as kl_B, is shown together with (J_x, J_y). The energies are measured from those of the ground states indicated by arrows. (a) Δ_{SAS} = 0.006, Δ_Z = 0.001. (b) Δ_{SAS} = 0.006, Δ_Z = 0.05. (c) Δ_{SAS} = 0.2, Δ_Z = 0.014. (d) Δ_{SAS} = 0.2, Δ_Z = 0.001. (e) Δ_{SAS} = 0.2, Δ_Z = 0.05. (f) Δ_{SAS} = 0.2, Δ_Z = 0.014.

should be noted that $k = 1.02/l_B$ states are two-fold degenerate because (0, 1) and (1, 0) are equivalent. **Figures 1(a)-(c)** represent the spectra at small $\Delta_{SAS} = 0.006$. Actually, in these figures the marks of the ground state are almost doubly degenerate, composed of symmetry and antisymmetry states. While from the spectra at relatively large $\Delta_{SAS} = 0.2$ in **Figures 1(d)-(f)**, we find that all the ground states become non-degenerate states. On the other hand, the spin polarizations of the ground states are determined by Δ_Z. As Δ_Z is equal to a small value of 0.001 in **Figure 1(a)** and **Figure 1(d)**, the ground states have the total spin $S_z = 0$, being the SU states. When Δ_Z becomes as large as 0.05 in **Figure 1(b)** and (e), the ground states turn out to be the SP states with $Sz = 2$. The ground states have $k = 0$, as implies that they are homogeneous states. Both SP and SU ground states are QH states, where the lowest excited states have nonzero energy gap: They compose SP and SU phases. When Δ_Z has an intermediate value of 0.014 as shown in **Figure 1(c)** and **Figure 1(f)**, there are several states with almost equivalent lowest gap energies but different S_z, thus they all may become the ground states in these crossover regions when Δ_Z is slightly changed.

We introduce the most important basis states (MIBSs) of the ground state to investigate the properties of them. We find that two degenerate ground states in **Figure 1(b)** have the same representative basis vectors in the MIBSs. They are {2f ↑ , 3f ↑ , 5f ↑ , 6f ↑ }, {2b ↑ , 3b ↑ , 5b ↑ , 6b ↑ }, {1f ↑ , 2f ↑ , 3f ↑ , 4f ↑ } and {1b ↑ , 2b ↑ , 3b ↑ , 4b ↑ }, with the amplitudes of (0.6279, 0.6269, 0.3250, 0.3245) and (0.6269, −0.6279, 0.3245, −0.3250) for two degenerate ground states, respectively. Although the absolute value of the amplitudes are almost equal, the signs of the second and the fourth components are opposite, implying that they represent the symmetry and antisymmetry states, respectively. This phenomenon generally appears in the other degenerate ground states when Δ_{SAS} is small.

Figure 2 demonstrates the energy gaps E_{gap} between the lowest two eigenstates as a function of Δ_{SAS} for several values of d in the $\nu = 2/3$ bilayer QH system for $\Delta_Z = 0.001$ and 0.05. The lowest two eigenstates are the symmetric and antisymmetric states. As expected, they are almost degenerate in the small Δ_{SAS} regions. With the increase of Δ_{SAS}, E_{gap} smoothly widen, implying that the degeneracy of two states is resolved gradually, and finally tend to saturation points where the energies of the antisymmetric states exceed those of excited states created on the symmetric states. On the other hand, we notice that, when d changes from 0 to 10, the degenerate regions expand gradually and get to the limits. It is probably because the interlayer Coulomb energies exponentially decrease when d increases, while the intralayer Coulomb energies are independent from d. It is conjectured that the large difference between the intralayer and interlayer Coulomb energies will increase the degeneracy of the ground states. The general features in **Figure 2(a)** and **Figure 2(b)** are similar, while the only difference between them is the values of E_{gap} at the saturation points at large Δ_{SAS}, resulting from different excited states.

We plot the image of E_{gap} in the $\Delta_{SAS\text{-}\Delta Z}$ plane with the choice of $d = 1.0$ in the

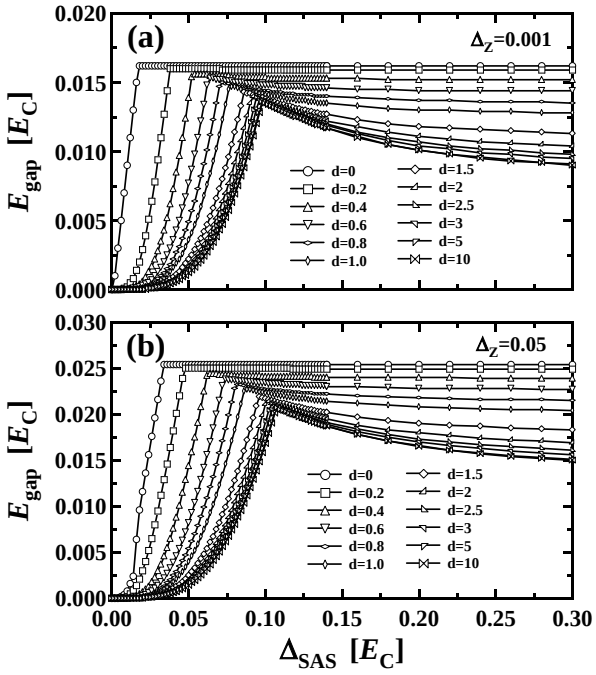

Figure 2. Energy gaps Egap between the lowest two eigenstates as a function of Δ_{SAS} for several values of d in finite size ν = 2/3 bilayer QH systems (a) When Δ_Z = 0.001; (b) When Δ_Z = 0.05. The energy and d are in units of $E_C = e^2/4\pi\varepsilon l_B$ and l_B, respectively.

right side of the vertical dotted line in **Figure 3(a)**, where E_{gap} represents the energy gap between the lowest first and second eigenstates for the non-degenerate ground states case. We also plot the image of E_{gapD} in the left side of the vertical dotted line in Figure 3(b), where E_{gapD} represents the energy gap between the second and third eigenstates for the degenerate ground states case. The SP and SU phases occupy the high- and low-Δ_Z regions with relative large E_{gap} (E_{gapD}) respectively. Because the phase transition between them is continuous in the finite size systems, in this paper, the crossover (CR) region is defined by the remaining part around the phase transition boundary where the values of E_{gap} (E_{gap}D) are less than one tenth of the average values of the E_{gap} (E_{gapD}) in the SP and SU phases. The solid lines in the **Figure 3(a)** and **Figure 3(b)** give the upper and lower limits of the CR regions, and the dashed lines between them indicate the spin-flipping positions (between S_z = 0 and S_z = 2). The points A-E plotted in the figure are the experimental results of the phase boundaries (from N. Kumada*et al*, Y. D. Zheng*et al*). The most significant feature in **Figure 3(a)** and **Figure 3(b)** is that, the SP-SU phase transition region (or the CR region) is limited in a narrow areawith Δ_Z from 0.009 to 0.014. Though the transition region slightly bends toward the low Δ_Z side when Δ_{SAS} increases, we can say generally it is only weakly dependent on Δ_{SAS}. This fact gives the reliable evidence that the SP-SU phase transitions are determined by the competition between Δ_Z and Δ_C. It should be emphasized that in the $\nu = 2/3$ system, because the electrons only occupy the symmetric level, the factor Δ_{SAS} representing the

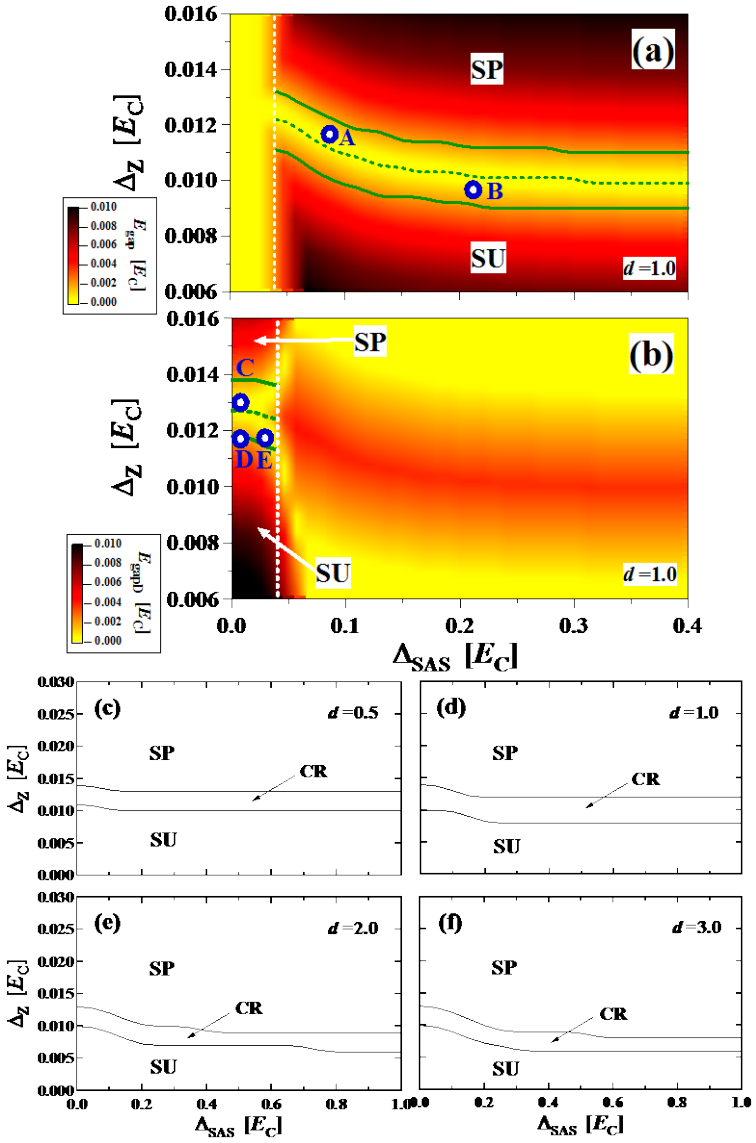

Figure 3. Image plot of energy gaps E_{gap} between the lowest first and second eigenstates (a) and E_{gapD} between second and third eigenstates (b) in the Δ_{SAS}-Δ_Z plane in finite size ν = 2/3 bilayer QH systems. Symbols SP, SU and CR denote the spin polarized, unpolarized phases and the crossover region, respectively. The solid lines give the upper and lower limits of the CR regions, and the dashed lines between them indicate the spin-flipping positions. The points A-E are the experimental results of the phase boundaries in the ν = 2/3 bilayer QH systems; (c)-(f) SP, SU and CR regions in the Δ_{SAS}-Δ_Z planes for several values of d: (c) d = 0.5; (d) d = 1.0; (e) d = 2.0; (f) d = 3.0. The energy and d are in units of $E_C = e^2/4\pi\varepsilon l_B$ and l_B, respectively.

energy gap between the symmetric and antisymmetric levels, will not affect the phase transition boundary. For this reason, the Δ_Z holds a nonzero value in the transition region, even if Δ_{SAS} vanishes. **Figures 3(c)-(f)** present the SP, SU phases and CR region in the Δ_{SAS}-Δ_Z plane for several values of d. When d changes from 0.5 to 3.0, the whole CR region slightly shifts to the low Δ_Z side, and arrives to a limit about 0.005. Qualitatively, d has no great influence on the

phase transition region.

4. Analytic Investigation Using an Exactly Solvable Model

The degeneracy of the ground states when Δ_{SAS} is small can be investigated analytically by a two-electron model in the SP phase. With the help of the symmetries mentioned previously, the H matrix of this model can be divided into nine independent blocks. We write down five basis vectors corresponding to the block with the J_y (J_x) value of 0 and the S_z value of 1 as $\varphi_1 = \hat{\mathbf{c}}^+_{1f\uparrow}\hat{\mathbf{c}}^+_{2f\uparrow}|0\rangle$, $\varphi_2 = \hat{\mathbf{c}}^+_{1f\uparrow}\hat{\mathbf{c}}^+_{2b\uparrow}|0\rangle$, $\varphi_3 = \hat{\mathbf{c}}^+_{1b\uparrow}\hat{\mathbf{c}}^+_{2f\uparrow}|0\rangle$, $\varphi_4 = \hat{\mathbf{c}}^+_{1b\uparrow}\hat{\mathbf{c}}^+_{2b\uparrow}|0\rangle$ and $\varphi_5 = \hat{\mathbf{c}}^+_{3f\uparrow}\hat{\mathbf{c}}^+_{3b\uparrow}|0\rangle$, which belong to the SP phase. Using the Hamiltonian in Equation (1), we obtain a 5 × 5 block matrix calculated by the basis vectors above as follows:

$$[H_{001}] = \begin{pmatrix} A_{1221}-A_{1212}-\Delta_Z & -(1/2)\Delta_{SAS} & -(1/2)\Delta_{SAS} & 0 & 0 \\ -(1/2)\Delta_{SAS} & B_{1221}-\Delta_Z & -B_{1212} & -(1/2)\Delta_{SAS} & B_{2133} \\ -(1/2)\Delta_{SAS} & -B_{1212} & B_{1221}-\Delta_Z & -(1/2)\Delta_{SAS} & -B_{1233} \\ 0 & -(1/2)\Delta_{SAS} & -(1/2)\Delta_{SAS} & A_{1221}-A_{1212}-\Delta_Z & 0 \\ 0 & B^*_{2133} & -B^*_{1233} & 0 & B_{3333}-\Delta_Z \end{pmatrix} \quad (3)$$

where A_{pqrs} ($\langle\phi_{pf},\phi_{qf}|V|\phi_{rf},\phi_{sf}\rangle$ or $\langle\phi_{pb},\phi_{qb}|V|\phi_{rb},\phi_{sb}\rangle$) and B_{pqrs}(= $\langle\phi_{pf},\phi_{qb}|V|\phi_{rb},\phi_{sf}\rangle$ or $\langle\phi_{pb},\phi_{qf}|V|\phi_{rf},\phi_{sb}\rangle$ represent the intralayer and interlayer Coulomb interaction energies, respectively. The subscripts p, q, r and s denote the momentum index in the y direction. $\phi_{j\mu}$ is the single-electron wave function in the LLL. A_{1221}, for instance, is the direct Coulomb energy between two electrons in sites 1 and 2, while A_{1212} is the exchange energy between them.

The block $[H_{001}]$ can be diagonalized analytically through the conventional method, and we derive all eigenvalues and eigenstates of the matrix characteristic equation $[H_{001}](A_{\varphi_1}\ A_{\varphi_2}\ A_{\varphi_3}\ A_{\varphi_4}\ A_{\varphi_5})^T = E(A_{\varphi_1}\ A_{\varphi_2}\ A_{\varphi_3}\ A_{\varphi_4}\ A_{\varphi_5})^T$. The five exact eigenvalues (E_1 - E_5) of the block $[H_{001}]$ are given by

$$E_1 = \frac{(A_{1221}-A_{1212}+B_{1221}-B_{1212})-\sqrt{\Delta_1}}{2}-\Delta_Z,\quad E_2 = A_{1221}-A_{1212}-\Delta_Z,$$

$$E_3 = \frac{(A_{1221}-A_{1212}+B_{1221}-B_{1212})+\sqrt{\Delta_1}}{2}-\Delta_Z,$$

$$E_4 = \frac{(B_{3333}+B_{1221}+B_{1212})-\sqrt{\Delta_2}}{2}-\Delta_Z,$$

$$E_5 = \frac{(B_{3333}+B_{1221}+B_{1212})+\sqrt{\Delta_2}}{2}-\Delta_Z, \quad (4a)$$

with

$$\Delta_1 = (A_{1221}-A_{1212}-B_{1221}+B_{1212})^2+4\Delta^2_{SAS},$$

$$\Delta_2 = (B_{3333}-B_{1221}-B_{1212})^2+8|B_{1233}|^2. \quad (4b)$$

Since the relationship $A_{1221}-A_{1212} < B_{1221}-B_{1212}$ holds always in the system, one obtains provided Δ_{SAS} = 0, exhibiting two degenerate ground states with

equivalent eigenvalues E_1 and E_2. The eigenstates in this case are simply $\hat{\mathbf{c}}^{+}_{1f\uparrow}\hat{\mathbf{c}}^{+}_{2f\uparrow}|0\rangle$ or $\hat{\mathbf{c}}^{+}_{1b\uparrow}\hat{\mathbf{c}}^{+}_{2b\uparrow}|0\rangle$ implying that electrons are restricted within one of the layers.

When Δ_{SAS} departures from zero, E_1 is also separated from E_2 taking a lower value. Thus, the degeneracy of the ground states is solved gradually. However, when Δ_{SAS} is sufficiently small, E_1 and E_2 are almost equal, and can be regarded as degenerate. In this case, the difference between E_1 and E_2 can be approximated by

$$|E_1 - E_2| = \Delta_{SAS}\left|\frac{\Delta_{SAS}}{A_{1221} - A_{1212} - B_{1221} + B_{1212}}\right|. \tag{5}$$

It is obvious that the degeneracy of the ground states is increased not only by the small Δ_{SAS} but also by the large difference between the intralayer and interlayer Coulomb energies, because $|E_1 - E_2|$ is in proportion to the product of Δ_{SAS} and the ratio of Δ_{SAS} and $\left|(A_{1221} - A_{1212}) - (B_{1221} - B_{1212})\right|$. Equation (5) reliably gives an analytic interpretation of the numerical results presented **Figure 2**. On the other hand, the eigenstates corresponding to E_1 and E_2 are expressed by

$$\Psi_{E_1} = a\left(\hat{\mathbf{c}}^{+}_{1f\uparrow}\hat{\mathbf{c}}^{+}_{2f\uparrow}|0\rangle + \hat{\mathbf{c}}^{+}_{1b\uparrow}\hat{\mathbf{c}}^{+}_{2b\uparrow}|0\rangle\right) + b_1\hat{\mathbf{c}}^{+}_{1f\uparrow}\hat{\mathbf{c}}^{+}_{2b\uparrow}|0\rangle + b_2\hat{\mathbf{c}}^{+}_{1b\uparrow}\hat{\mathbf{c}}^{+}_{2f\uparrow}|0\rangle + b_3\hat{\mathbf{c}}^{+}_{3f\uparrow}\hat{\mathbf{c}}^{+}_{3b\uparrow}|0\rangle,$$

$$\Psi_{E_2} = \left(\sqrt{2}/2\right)\left(\hat{\mathbf{c}}^{+}_{1f\uparrow}\hat{\mathbf{c}}^{+}_{2f\uparrow}|0\rangle - \hat{\mathbf{c}}^{+}_{1b\uparrow}\hat{\mathbf{c}}^{+}_{2b\uparrow}|0\rangle\right). \tag{6}$$

For sufficiently small Δ_{SAS}, since coefficients $b_1 - b_3$ are all close to zero, the two degenerate ground states with energies E_1 and E_2 are symmetric and anti-symmetric states, as argued previously.

5. Conclusion

In summary, we have studied a typical bilayer FQH system with finite size using the numerical and analytic methods and provided evidential quantitative results. We have found some basic features of the ground states at the layer balanced point in the $\nu = 2/3$ bilayer QH systems taking advantage of the ED calculations and the analysis of an exactly solvable two-electron system. When Δ_{SAS} is small, the degeneracy of the ground states occurs depending on the relative strength of the intralayer and interlayer Coulomb energies. SP-SU phase transitions are continuous in the finite size systems, and are determined by the competition between Δ_Z and Coulomb energy Δ_C, almost not affected by Δ_{SAS}. These features exhibit the essential difference between the $\nu = 2/3$ bilayer FQH systems and the $\nu = 2$ bilayer IQH systems, and the peculiar characteristics generally existing in most bilayer FQH systems. The ED numerical method and the exact-solution method employed in this paper also can be considered to be valuable in studies of other bilayer FQH systems.

Acknowledgements

This research was supported in part by Grants-in-Aid for the basic research and development of Mitsubishi Electric (China) Company Limited.

References

[1] Klitzing, K.V., Dorda, G. and Pepper, M. (1980) *Phys. Rev. Lett.*, **45**, 494. https://doi.org/10.1103/PhysRevLett.45.494

[2] Tsui, D.C., Stormer, H.L. and Gossard, A.C. (1982) *Phys. Rev. Lett.*, **48**, 1559. https://doi.org/10.1103/PhysRevLett.48.1559

[3] Laughlin, R.B. (1983) *Phys. Rev. Lett.*, **50**, 1395. https://doi.org/10.1103/PhysRevLett.50.1395

[4] Halperin, B.I. (1984) *Phys. Rev. Lett.*, **52**, 1583. https://doi.org/10.1103/PhysRevLett.52.1583

[5] Jain, J.K. (1989) *Phys. Rev. Lett.*, **63**, 199. https://doi.org/10.1103/PhysRevLett.63.199

[6] Das Sarma, S. and Pinczuk, A. (editor) (1997) Perspectives in Quantum Hall Effects. Wiley, New York.

[7] Girvin, S.M. (1999) arXiv: cond-mat/9907002v1

[8] Zheng, L., Radtke, R.J. and Das Sarma, S. (1997) *Phys. Rev. Lett.*, **78**, 2453. https://doi.org/10.1103/PhysRevLett.78.2453

[9] Das Sarma, S., Sachdev, S. and Zheng, L. (1998) *Phys. Rev. B*, **58**, 4672. https://doi.org/10.1103/PhysRevB.58.4672

[10] MacDonald, A.H., Rajaraman, R. and Jungwirth, T. (1999) *Phys. Rev. B*, **60**, 8817. https://doi.org/10.1103/PhysRevB.60.8817

[11] Brey, L., Demler, E. and Das Sarma, S. (1999) *Phys. Rev. Lett.*, **83**, 168. https://doi.org/10.1103/PhysRevLett.83.168

[12] Burkov, A.A. and MacDonald, A.H. (2002) *Phys. Rev. B*, **66**, Article ID: 115323.

[13] Lopatnikova, A., Simon, S.H. and Demler, E. (2004) *Phys. Rev. B*, **70**, Article ID: 115325.

[14] Demler, E. and Das Sarma, S. (1999) *Phys. Rev. Lett.*, **82**, 3895. https://doi.org/10.1103/PhysRevLett.82.3895

[15] Yang, K. (1999) *Phys. Rev. B*, **60**, 15578. https://doi.org/10.1103/PhysRevB.60.15578

[16] Schliemann, J. and MacDonald, A.H. (2000) *Phys. Rev. Lett.*, **84**, 4437. https://doi.org/10.1103/PhysRevLett.84.4437

[17] Yoshioka, D., Halperin, B.I. and Lee, P.A. (1983) *Phys. Rev. Lett.*, **50**, 1219. https://doi.org/10.1103/PhysRevLett.50.1219

[18] Yoshioka, D. (1984) *Phys. Rev. B*, **29**, 6833. https://doi.org/10.1103/PhysRevB.29.6833

[19] Haldane, F.D.M. (1985) *Phys. Rev. Lett.*, **55**, 2095. https://doi.org/10.1103/PhysRevLett.55.2095

[20] Haldane, F.D.M. and Rezayi, E.H. (1985) *Phys. Rev. Lett.*, **54**, 237. https://doi.org/10.1103/PhysRevLett.54.237